The Journal of Chemical Physics

Neutrondiffraction study of Ho2C at 4–296 K

Masao Atoji

Citation: J. Chem. Phys. **74**, 1893 (1981); doi: 10.1063/1.441280
View online: http://dx.doi.org/10.1063/1.441280
View Table of Contents: http://jcp.aip.org/resource/1/JCPSA6/v74/i3
Published by the American Institute of Physics.

Neutron-diffraction study of Ho_2C at 4–296 K [a)]

Masao Atoji

Chemistry Division, Argonne National Laboratory, Argonne, Illinois 60439
(Received 26 August 1980; accepted 15 October 1980)

By neutron powder diffraction, trigonal Ho_2C has been shown to become ferromagnetic below 100 K. The paramagnetic scattering indicates the free Ho^{3+}-ion moment, while the saturation moment in the ferromagnetic phase is 7.16 Bohr magnetons (72% of the free-ion moment), showing a sizeable crystal-field effect. The preferential crystallite orientation induced by the applied magnetic field has shown that the ordered moments are aligned parallel to the [104] axis which corresponds to the [100] axis of the high-temperature cubic modification. The previously proposed HoN-type magnetic ordering is not compatible with our results. The residual, disordered moments exhibit a ferromagnetic short-range order superposing on the ferromagnetic long-range order. Crystallographic-structure data at 296 and 4 K are also presented.

I. INTRODUCTION

The rare earth (RE) and carbon system[1] contains the hypocarbides (REC_x with $0.25<x<0.65$ and RE_2C),[2,3] the dicarbide (REC_2), and the sesquicarbide (RE_2C_3). We have carried out neutron-diffraction studies of practically all the accessible REC_2[4] and RE_2C_3,[5] and have been working on the hypocarbide series. We have determined the crystal structures of the trigonal Y_2C and the cubic $YC_{0.43}$. The transformation mechanism between the trigonal and cubic structures was revealed by using a single crystal in which the transient state in the midst of the phase transition was arrested.[6] We also found that Tb_2C[7] has a magnetic interaction stronger than the Tb metal and exhibits a moment alignment which is unique in the RE_2C series.

The neutron-diffraction studies of Ho_2C carried out by Lallement[2] and Bacchella *et al.*[3] gave the following results: Ho_2C is trigonal with the hexagonal unit cell of $a=3.556(7)$ and $c=17.70(1)$ at room temperature, containing three Ho_2C units; an anti-$CdCl_2$ type structure with the space group D^5_{3d}-$R\bar{3}m$; the atomic coordinates (0, 0, 0; 2/3, 1/3, 1/3; 1/3, 2/3, 2/3) $\pm(0, 0, z)$ with $z=0.256(1)$ and $z=0$ for Ho and C, respectively[3]; and the temperature-factor coefficient $2B=0.64$ Å^2. Lallement has also reported a neutron-diffraction pattern of Ho_2C at 4 K and postulated its ordered magnetic structure as a HoN-type retarded ferromagnet.[8] The Ho_2C study of Lallement also includes the temperature dependency of magnetization using neutron data, the magnetic susceptibility, the electrical resistivity, the thermoelectric power, and the electronic specific heat. The first four measurements gave the Curie temperatures of 100, 90, 90, and 100 K.

We have refined the crystal structure of Ho_2C at 296 K and have determined its structure parameters at 4 K. We found that the ordered magnetic structure is quite different from that postulated by Lallement.[2] We have also carried out new measurements on the magnetic-moment value, the temperature dependency of magnetization, the moment direction, and the magnetic diffuse scattering. The experimental error is the standard deviation of the least significant digit as given in parentheses after the mean value.

II. EXPERIMENTAL AND CRYSTALLOGRAPHIC

The sample was prepared by arc melting a compressed mixture of holmium-metal filings (99.9% pure) and spectroscopic-grade graphite powders. The product is metallic gray and is brittle enough to be crushed into powders. It decomposes slowly in moist air, liberating hydrogen and methane gases.[9,10] Chemical analysis of the arc-melted boules gave the molar ratio Ho : C $=2.00(5):1.00(5)$. Both neutron and x-ray diffraction patterns showed no detectable impurity peaks.

The neutron reflections (Fig. 1) established the hexagonal-lattice parameters as follows: $a=3.556(6)$ and $c=17.70(1)$ at 296 K, and $a=3.550(8)$ and $c=17.67(4)$ at 4 K. Hence, the linear thermal-expansion coefficients are 6×10^{-6} deg^{-1} for both the a and c axes, exhibiting no abnormally large magnetostriction. The molar volumes for Ho_2C are 64.6(3) and 64.3(3) Å^3, and the calculated densities are 8.78(3) and 8.83(4) g cm^{-3} at 296 and 4 K, respectively.

The nuclear intensities at 297 K gave $z=0.2564(8)$ for Ho and the temperature-factor coefficient as $2B=1.8(3)$ Å^2. The resultant calculated intensities are compared with the observed values in Table I, where the agreement factor $R=\sum|I_0-I_c|/\sum I_0$ is 1.8%. The nuclear-scattering lengths used are $b(\mathrm{Ho})=0.85$ and $b(C)=0.665$, both in 10^{-14} m.[11]

The crystal structure is depicted in Fig. 2, where the interatomic bonding distances at 4 K are Ho(I)–3Ho(III) $=3.416(15)$, Ho(I)–6Ho(II) $=3.550(8)$, Ho(I)–3Ho(IV) $=3.76(3)$, C–6Ho $=2.46(1)$, and C–6C′ $=3.550(8)$. The Ho(I)–Ho(III) bond across the carbon layer is considerably shorter than the Ho(I)–Ho(IV) bond across the vacant layer. For comparison, the first-neighbor distances in the Ho metal are 3.577 Å in the hexagonal basal plane and 3.486 Å across the hexagonal layers. These Ho–Ho distances indicate that the carbon atoms strengthen the metallic bond in Ho_2C, while a reverse relation has been found in most transition-metal carbides.[6]

III. MAGNETIC STRUCTURE

The coherent reflections in the ferromagnetic phase showed no broadening in their peak profiles (Fig. 1),

[a)] Work performed under the auspices of the Office of Basic Energy Sciences, Division of Materials Sciences, U. S. Department of Energy.

 0021-9606/81/031893-05$01.00

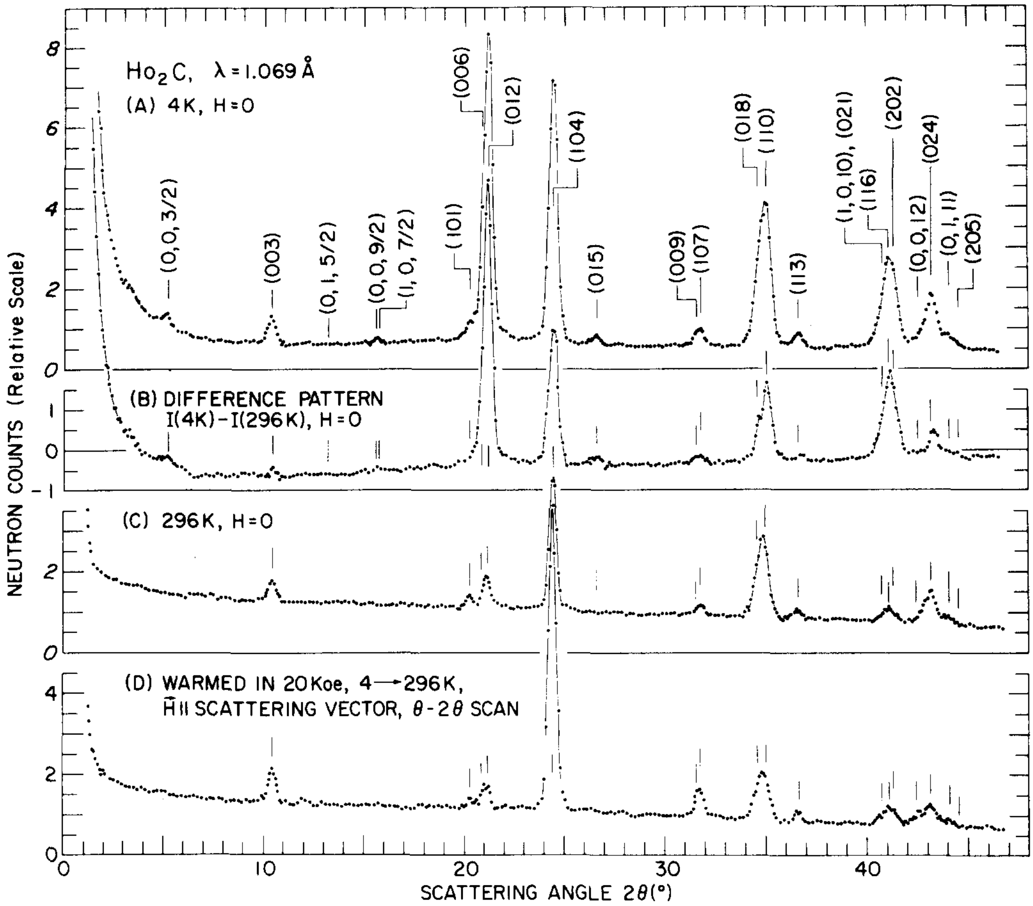

FIG. 1. Neutron-powder diffraction patterns of Ho_2C at 4 and 296 K in the zero magnetic field are given in (A) and (C), respectively. Pattern (B) is obtained by subtracting (C) from (A) and contains only the coherent and incoherent magnetic scattering. Pattern (D) was obtained by the $\theta-2\theta$ scan of the preferential crystallite orientation induced in the ferromagnetic phase by the magnetic field applied parallel to the scattering vector. The comparison between (C) and (D) leads to the ordered moment direction being parallel to the [104] axis. Several forward reflections of a magnetic superlattice (l = half-integer) are also indexed in (A).

contrary to the HoN-type magnetic ordering.[2,8] The magnetic coherent intensities [(B) of Fig. 1] were therefore analyzed using a commensurate-lattice formula

$$I_{\text{calc.}}(\text{mag.}) = \left(\frac{e^2\gamma}{2mc^2}\right)^2 jLf_m^2 F_m^2 (gJ)^2 \exp\left[-2B\left(\frac{\sin\theta}{\lambda}\right)^2\right] \times[\sin^2\psi - \tfrac{1}{2}(3\sin^2\psi - 2)\sin^2\phi] , \qquad (1)$$

where the reported equation[12] has been modified so that the variable contribution can be evaluated independently; γ is the neutron magnetic moment in nuclear Bohr magnetons; j is the multiplicity factor; L is the Lorenz factor; f_m is the magnetic-form factor[13]; F_m is the magnetic-structure factor and is equal to $\cos 2\pi z(\text{Ho})$ with $z(\text{Ho}) = 0.2547$; gJ is the ordered moment; $2B = 0.4$ Å^2 at 4 K; ψ is the angle between the c axis and the scattering vector; and ϕ is the angle between the c axis and the moment direction. The direction of the basal-plane component of the moment cannot be determined by the neutron-powder method.[12]

In comparison with the observed intensities at 4 K, the calculated intensities are very insensitive to variation in ϕ, as shown in Table II. The agreement factors are 2.1% and 1.8% for $\phi = 0°$ and 55.2°, respectively. Correspondingly, the resultant ordered moment is practically independent of the ϕ variation and gives $gJ = 7.16(8)$ μ_B, which is 72% of the free ion value of 10 μ_B. Lallement[2] has given $gJ = 5-6$ μ_B at 4 K, based on the HoN-type magnetic structure.[8] Lallement's data, however, can be interpreted more reasonably on the basis of our structure and the wavy diffuse scattering described below.

The moment direction in a ferromagnet can be uniquely determined by means of the preferential crystallite

TABLE I. Observed and calculated nuclear intensities in 10^{-26} m^2 per 0.5 Ho_2C at 296 K.

Indices	$I_{\text{calc.}}$		$I_{\text{obs.}}$	Indices	$I_{\text{calc.}}$		$I_{\text{obs.}}$
003	22.8		18.1	113	10.4		10.4
101	8.3		7.8	1,0,10	4.4	22.3	22.4
006	7.2	29.9	29.6	021	1.9		
012	22.7			116	10.4		
104	87.8		90.8	202	5.6		
015	1.4		<1.6	0,0,12	7.8	43.8	43.6
009	0.0	12.0	11.6	024	26.5		
107	12.0			0,1,11	9.0		
018	40.1	82.3	85.3	205	0.5		
110	42.2						

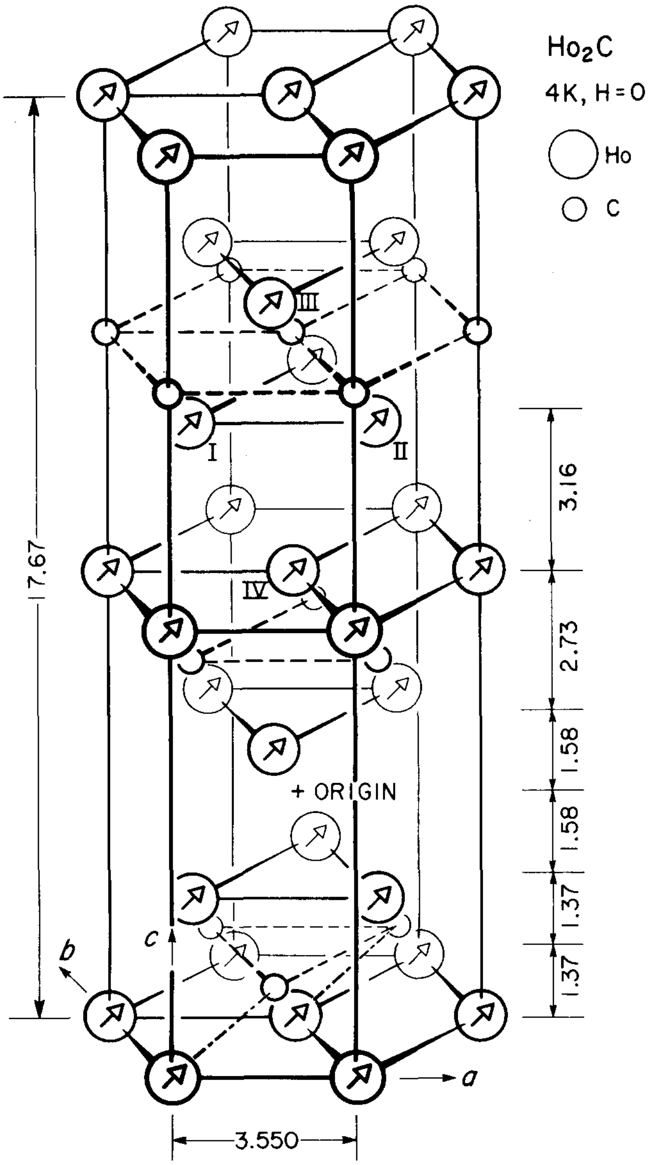

FIG. 2. Schematic representation of the crystal and magnetic structures of Ho_2C. The origin is placed at (0, 0, 1/2). Pertinent interlayer distances are given in Å. The arrows represent the moment directions which are parallel to the [104] axis and approximately parallel to the Ho–C bond as shown by semi-broken lines near the bottom layer.

orientation induced by the applied magnetic field.[14] The net moment of the crystallite tends to align in the direction of the applied field. The resultant preferred orientation axis can be determined by the $\theta-2\theta$ scan with the magnetic field applied parallel to the scattering vector. However, the effect of the preferred orientation on the nuclear intensity is quite different from that on the magnetic intensity. Hence, the preferred orientation is usually induced in the ferromagnetic phase, and then the intensities are collected in the paramagnetic phase in order to eliminate the coherent magnetic intensity. In practice, because of often unavoidable vibrational disturbance on powder packing in the experimental procedures, it is more convenient to carry out the warming process in the applied magnetic field. The diffraction pattern thereby obtained is shown in (D) of Fig. 1. Obviously, the moment direction is the [104] axis, which

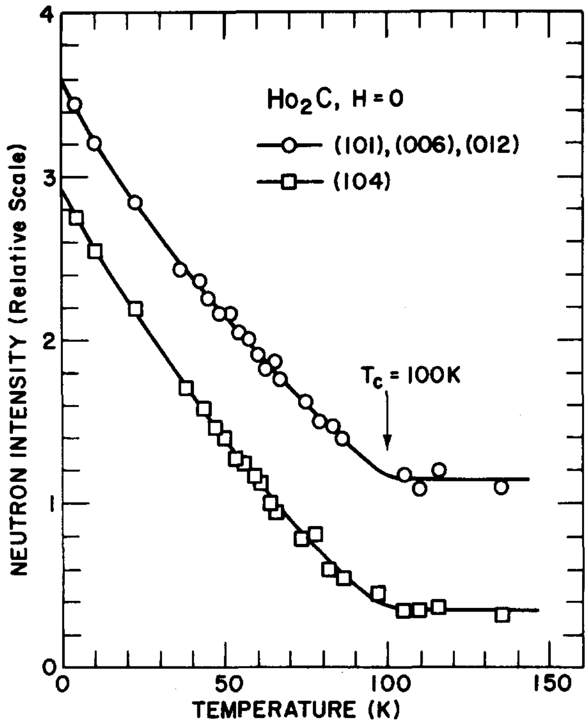

FIG. 3. Temperature dependence of the integrated magnetic intensity of the peak consisting of the (101), (006), and (012) reflections and that of the (104) reflection. Both sets gave T_c = 100(2) K.

corresponds to the [100] axis of the high-temperature cubic modification and is approximately parallel to the Ho–C bond (see Fig. 2). Diffraction intensities for preferred orientation in a hexagonal case have been formulated by Pesonen *et al.*[15]

The temperature dependencies of the integrated intensities of the representative magnetic reflections are shown in Fig. 3, from which the Curie temperature

TABLE II. Observed and calculated intensities of nuclear and magnetic reflections in 10^{-26} cm^2 per 0.5 Ho_2C at 4 K. The calculated magnetic intensities are given for the ordered moments parallel to the c axis ($\phi = 0°$) and to the [104] axis ($\phi = 55.2°$).

Indices	$I_{calc.}$ (nucl.)	$I_{calc.}$ (mag.) $\phi = 0°$	$I_{calc.}$ (mag.) $\phi = 55.2°$	$I_{calc.}$ (total) $\phi = 0°$	$I_{calc.}$ (total) $\phi = 55.2°$	$I_{obs.}$
003	23.0	0	4.2	23	27	24
101	8.6	0.5	0.3			
006	7.4	0	58.2	276	274	279
012	23.6	235.8	175.6			
104	92.4	123.5	122.1	216	215	214
015	1.5	3.4	4.0	5	6	7
009	0.0	0	2.7	16	21	20
107	13.1	2.9	4.9			
018	44.5	22.6	44.4	185	183	183
110	47.0	71.4	47.3			
113	11.7	1.7	1.2	13	13	13
1,0,10	5.1	9.5	25.5			
021	2.2	0.1	0.1	138	135	136
116	12.1	60.7	55.1			
202	6.5	41.9	28.6			
0,0,12	9.2	0	7.0			
024	31.2	32.8	24.4	87	88	83
0,0,11	10.6	1.4	4.4			
205	0.6	1.1	0.9			

(T_c) was determined to be 100(2) K, which is in excellent agreement with Lallement's results.[2] Temperature dependence of the spontaneous magnetization on a normalized scale (Fig. 4) is represented approximately by $M(T) = M(0)\,[1-(T/T_c)^{2/3}]$, where $M(T)$ is proportional to the ordered moment at T. Lallement's data[2] are represented by $M(T) = M(0)\,[1-(T/T_c)]$, which is significantly different from ours. This discrepancy is probably due to the difficulty in determining the background level of reflection, since the magnetic diffuse scattering gives rise to a temperature-dependent wavy background. This aspect was carefully treated in our data processing. In Tb_2C,[7] we obtained a still different relation $M(T) = M(0)\,[1-(T/T_c)^2]$. In all these RE_2C cases, the Brillouin curve for $(g-1)J$ is definitely not in accordance with the observed values (Fig. 4).

The magnetic diffuse scattering at 296 K (Fig. 4) gave the effective Bohr magneton number of $\mu_{eff} = 10.2(2)\ \mu_B$, which agrees with $\mu_{eff} = 10.61\ \mu_B$ of the free Ho^{3+} ion. A small hump around $\sin\theta = 0$ is probably caused by a weak ferromagnetic short-range ordering. The humpy modulation of the scattering curve becomes more pronounced at lower temperatures and persists down to 1.6 K. This implies that the ferromagnetic short-range ordering coexists with the ferromagnetic long-range ordering.[16]

The magnetic diffuse scattering at 4 K was analyzed using a first-order approximation of the short-range order formula[17]

$$\frac{d\sigma}{d\omega} = \frac{2}{3}\left(\frac{e^2\gamma}{2mc^2}\right)^2 \mu_{eff}^2 f_m^2 \left(1 - \frac{2\mu_{eff}^2}{3kT}\sum_n J_n z_n \frac{\sin X_n}{X_n}\right) , \tag{2}$$

where $d\sigma/d\omega$ is the differential-scattering cross section in barn/sr/Ho^{3+}; the first term represents the paramagnetic scattering, and the second term represents the short-range-order effect; μ_{eff} is the effective Bohr magneton number of the disordered moment in μ_B; J_n is proportional to the exchange interaction between a given atom and the nth neighboring atom; z_n is the number of the nth neighbors; $X_n = 4\pi r_n \sin\theta/\lambda$; and r_n is the nth neighboring distance. Other notations are explained in Eq. (1).

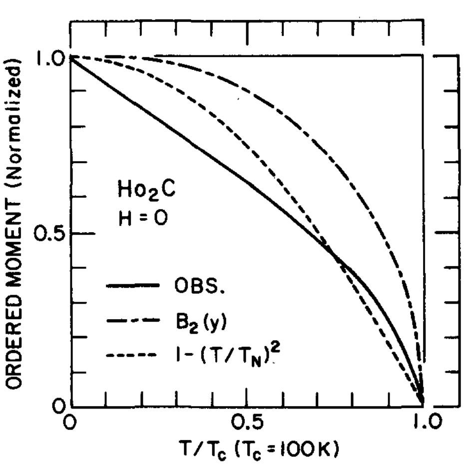

FIG. 4. Reduced magnetic moment as a function of reduced temperature T/T_c. The Brillouin curve for $(g-1)J = 2$ is shown by a broken line. The Tb_2C case is represented approximately by $[1-(T/T_c)^2]$, which is shown by a broken line for comparison.

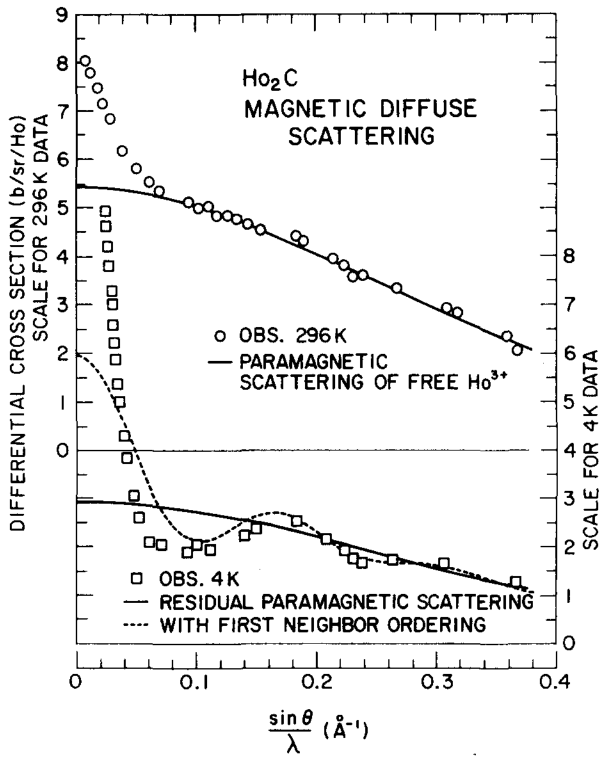

FIG. 5. Observed diffuse magnetic-scattering cross sections of Ho_2C at 297 and 4 K are given by open circles and open squares, respectively. The calculated curves for the incoherent magnetic scattering in the disordered moments are shown, using solid lines. The calculated scattering in the disordered moments with a ferromagnetic first-neighbor short-range ordering is given by a broken line.

The median curve of the observed data was fitted approximately by the first term of Eq. (2) with $\mu_{eff} = 7.8(2)\ \mu_B$, which corresponds to $[(\mu_{eff}\text{ for the free ion})^2 - (\text{ordered moment})^2]^{1/2} = (10.61^2 - 7.16^2)^{1/2} = 7.83\ \mu_B$. Although no unique curve fitting was obtained in the short-range order terms, an approximate first-neighbor interaction curve is shown in Fig. 5 for illustration using a ferromagnetic $J_1 = -0.0056k$. A very strong intensity in the vicinity of $\sin\theta = 0$ consists of all the ferromagnetic short-range orderings at the maximum positive values and an intense coherent ferromagnetic reflection at $h = k = l = 0$.

The diffraction pattern at 4 K (Fig. 1) shows a few, weak superlattice reflections, which could not be attributed to the crystal-structure change or to the impurities. If these reflections originated in the antiferro- or ferromagnetic structure, then the ordered moment would have mostly the basal-plane component having 0.5–1.5 μ_B with the repetition period of $2c$. The maximum possible ordered moment is therefore $(7.16^2 + 1.4^2)^{1/2} = 7.3\ \mu_B$. Neutron-diffraction studies of Dy_2C and $ErC_{0.6}$, as well as a refined work on Tb_2C, are in progress, and all these results in the RE_2C series will be discussed cumulatively elsewhere.

[1]F. H. Spedding, K. Gschneidner, Jr., and A. H. Daane, J. Am. Chem. Soc. 80, 4499 (1958).
[2]R. Lallement, Centre d'Etudes Nucléaires de Fonteney-aux-Roses Rapport CEA-R 3043 (1966).
[3]G. L. Bacchella, P. Meriel, M. Pinot, and R. Lallement, Bull. Soc. Fr. Mineral. Cristallogr. 89, 226 (1966).
[4]M. Atoji, J. Chem. Phys. 57, 2410 (1972), and references therein.
[5]M. Atoji, J. Solid State Chem. 26, 51 (1978), and references therein.
[6]M. Atoji and M. Kikuchi, J. Chem. Phys. 51, 3863 (1969); Argonne National Laboratory Report ANL-7441 (1968).
[7]M. Atoji, J. Chem. Phys. 51, 3872 (1969).
[8]H. R. Child, M. K. Wilkinson, J. W. Cable, W. C. Koehler, and E. O. Wollan, Phys. Rev. 131, 922 (1963).
[9]H. J. Svec, J. Capellen, and F. E. Saafeld, J. Inorg. Nucl. Chem. 26, 721 (1964).
[10]J. S. Anderson, N. J. Clark, and I. J. McColm, J. Inorg. Nucl. Chem. 30, 105 (1968).
[11]G. E. Bacon, Acta Crystallogr. Sect. A 28, 357 (1972).
[12]G. Shirane, Acta Crystallogr. 12, 282 (1959).
[13]M. Blume, A. J. Freeman, and R. E. Watson, J. Chem. Phys. 37, 1245 (1962); 41, 1878 (1964).
[14]M. Atoji, I. Atoji, C. Do-Dinh, and W. E. Wallace, J. Appl. Phys. 44, 5096 (1973).
[15]A. Pesonen, M. Järvinen, and K. Kurki-Suonio, Phys. Fenn. 8, 81 (1973).
[16]G. T. Trammell, Phys. Rev. 131, 932 (1963).
[17]M. Slotnick, Phys. Rev. 83, 1226 (1951).